Fruit Research

ARTICLE

Open Access

https://doi.org/10.48130/FruRes-2023-0043

Fruit Research **2023**, 3:43

Ectopic expression of an apple ABCG transporter gene *MdABCG25* increases plant cuticle wax accumulation and abiotic stress tolerance

Min-Min Zhou[1], Zi-Han Yu[1], Huai-Na Gao[1], Meng-Ru Li[1], Ya-Ting Wu[1], Hai-Yang Li[1], Tao Wang[2], Yan-Hui Lv[1*], Han Jiang[1*] and Yuan-Yuan Li[1*]

[1] *National Key Laboratory of Wheat Improvement, Shandong Collaborative Innovation, Center of Fruit & Vegetable Quality and Efficient Production, National Research, Center for Apple Engineering and Technology, College of Horticulture Science and Engineering, Shandong Agricultural University, Tai-An 271018, Shandong, China*

[2] *Tai'an Institute for Food and Drug Control, Tai-An 271000, Shandong, China*

* Corresponding authors, E-mail: 13165381596@163.com; jh12307@163.com; liyy0912@163.com

Abstract

A number of enzymes and transcription factors involved in cuticular wax biosynthesis have been identified in numerous plant species. The pathway of wax biosynthesis is relatively definite. The molecular basis of cuticular wax deposition is still unclear, especially the transport mechanism of cuticular wax from endoplasmic reticulum (ER) to the cell wall. It has been found that the ABCG transporter family is involved in the wax export process in some model plants. However, whether ABCG transporters participate in wax transport in apple is unknown. In this study, *MdABCG25*, encoding an ABCG transporter, was isolated from apple (*Malus domestica* Brokh.). *MdABCG25*, containing an AAA domain and an ABC2_membrane domain, is highly expressed in apple pericarp and induced by drought, salt and ABA conditions. The heterologous expression of *MdABCG25* in *Arabidopsis* leads to an increasing cuticular wax accumulation of stems and leaves. The epidermal permeability, water loss rate and chlorophyll extraction rate of *MdABCG25* transgenic *Arabidopsis* were decreased. The expression of *MdABCG25* improved the drought and salt tolerance of apple calli and *Arabidopsis*.

Citation: Zhou MM, Yu ZH, Gao HN, Li MR, Wu YT, et al. 2023. Ectopic expression of an apple ABCG transporter gene *MdABCG25* increases plant cuticle wax accumulation and abiotic stress tolerance. *Fruit Research* 3:43 https://doi.org/10.48130/FruRes-2023-0043

Introduction

The epidermis cuticle of the plant, composed of cutin and wax, is a hydrophobic barrier that covers the surface of all land plants. Plant epidermal wax has the functions of preventing non-stomatal water loss, preventing ultraviolet damage, maintaining surface cleaning and waterproofing, resisting the invasion of diseases and pests, etc., which plays a very important role in adapting to the external environment[1−3]. At present, the metabolic pathway of plant wax biosynthesis has been basically clarified through the studies of various plant wax biosynthesis including Arabidopsis, rice and tomato. However, the transport mechanism of epidermis wax is not clear.

The synthesized wax is transported from the endoplasmic reticulum (ER) to the plasma membrane (PM), then to the apoplast, and then from the apoplast to the epidermal cuticle through trans-cell wall transport, where it is assembled into epidermal wax crystals. Previous studies have shown that ABCG transporter is necessary for the normal wax transport of plants. The absence of *ABCG7* in moss (*Physcomitrella patens*) exhibited severely deficient in cuticular wax and less tolerant to drought stress[4]. *AtABCG12/AtCER5*, the first cloned ABCG transporter from plants, was proved to be involved in the cuticle wax transport[5]. Its absence leads to the deposition of wax components in the cytoplasm and a decrease in the amount of wax in the epidermis. *AtABCG13* is essential for the transport of flower cuticular lipids[6]. *OsABCG26* and *OsABCG15* genes cooperate to regulate the transport of wax components in the outer wall of rice pollen[7]. *AtABCG32* and its homologous genes, barley *HvABCG31* and maize *Glossy13*, are involved in the extracellular transport of various wax components[8−10]. However, it is unknown whether ABCG transporters have the function of wax transport in apple.

In this study, we isolated an ABCG transporter *MdABCG25* from apple, and obtained transgenic *Arabidopsis* plants stably expressing *MdABCG25* and *MdABCG25* transgenic apple calli. Subsequently, the epidermal ultrastructure and permeability, amounts of cuticular wax and resistance to abiotic stresses of transgenic lines were examined compared with wild type. Ultimately, we found that *MdABCG25* was involved in the transport of cuticular wax, reduced water loss, improved the response to drought and salt conditions.

Our study reveals a new molecular regulation mechanism of cuticular wax transport in apple, providing a candidate gene for studying the formation of apple wax layer and improving apple gloss quality.

Materials and methods

Plant materials and growth conditions

All kinds of apple tissues, including root, leaf, flower, fruit, and pericarp, were collected from eight-year-old 'Royal Gala' apple trees.

Tissue-cultured 'Royal Gala' apple seedlings were subcultured at 30-d intervals on Murashige and Skoog medium (4.43 g·L^{-1} MS and 30 g·L^{-1} sucrose) with 0.3 mg·L^{-1} 6-benzylaminopurine

(6-BA), 0.2 mg·L^{-1} 3-indoleacetic acid (IAA), 0.1 mg·L^{-1} gibberellin A3 (GA3) and 0.8% agar under a 16 h light/8 h dark photoperiod at 26 °C with 60% relative humidity. The seedlings were treated with 10% polyethylene glycol (PEG) 6000, 100 mmol·L^{-1} NaCl for 0, 1, 2, 3, 6, or 12 h, or 100 μmol·L^{-1} ABA for 0, 3, 6, 9, 12, or 24 h.

'Orin' apple calli were subcultured on MS medium with 0.4 mg·L^{-1} 6-benzylaminopurine (6-BA), 1.5 mg·L^{-1} 2, 4-dichlorophenoxyacetic acid (2,4-D) and 0.8% agar for 20 d in the dark at 26 °C.

Arabidopsis, including ecotype Columbia (Col-0) and *MdABCG25* ectopic expression transgenic lines (*MdABCG25*-OE-1, *MdABCG25*-OE-2, *MdABCG25*-OE-3), and tobacco (*Nicotiana benthamiana*) seedings were grown on 1/2 MS medium under 16 h light/8 h dark photoperiod at 26 °C and 60% relative humidity. Transgenic *Arabidopsis* seeds were screened in 1/2 MS medium containing 50 mg·L^{-1} Kanamycin. Positive transgenic plants were detected by polymerase chain reaction (PCR) and real-time quantitative PCR (RT-qPCR). The phenotypic analysis was conducted using the homozygous T3 plants obtained after three consecutive generations of screening. Seeds of the Col-0 and *MdABCG25*-OE transgenic lines were vernalized with low temperature (4 °C) for 3 d after sowing on 1/2 MS medium. Then, the 4-day-old seedlings with uniform sizes were transferred to 1/2 MS, 1/2 MS with 6% PEG 6000, 1/2 MS with 100 mmol·L^{-1} NaCl or 1/2 MS with 30 μmol·L^{-1} ABA medium. The root lengths and fresh weight of the seedlings were measured using ImageJ-win64 software and one in 10,000 electronic balance after 2 weeks.

Bioinformatics analysis of the *MdABCG25* gene

Basic information about the *MdABCG25* sequence were obtained from the NCBI database (www.ncbi.nlm.nih.gov/), namely number of base pairs (bp), number of amino acids (aa), number of exons and introns, chromosome location, and analysis of conserved domains. The molecular weight, isoelectric point (pI), instability index, and aliphatic index were predicted using ProtParam website (https://web.expasy.org/protparam/). The hydropathicity were predicted using ProtScale website (http://web.expasy.org/protscale). The secondary and tertiary structures were predicted using Phyre2 website (www.sbg.bio.ic.ac.uk/phyre2/html/page.cgi?id=index), PSIPRED website (http://bioinf.cs.ucl.ac.uk/psipred/) and SWISS-MODEL website (https://swissmodel.expasy.org/interactive). The transmembrane domains were predicted using TMHMM2.0 website (www.cbs.dtu.dk/services/TMHMM/). The signal peptides were predicted using SignalP - 5.0 website (https://services.healthtech.dtu.dk/service.php?SignalP-5.0). The serine, threonine and tyrosine phosphorylation sites were predicted using NetPhos 3.1 website (https://services.healthtech.dtu.dk/service.php?NetPhos-3.1).

Phylogenetic analysis, multiple sequence alignment of MdABCG25 proteins and conserved domain analysis

ABCG25 proteins of 17 different plants were obtained from the NCBI database (www.ncbi.nlm.nih.gov/) and constructed genetic evolutionary trees using MEGA_64 software. DNAMAN were used for sequence alignment. The conserved domains were predicted using SMART (http://smart.embl-heidelberg.de/). The bootstrap method was used to identify the evolutionary pathway, and 1,000 repeats were generated to verify the results.

Analysis of the *MdABCG25* promoter

The *cis*-acting elements in the *MdABCG25* promoter (2,000 bp upstream of the transcription start site) were identified using PlantCARE website (http://bioinformatics.psb.ugent.be/webtools/plantcare/html/).

Construction of the *MdABCG25* expression vector and genetic transformation into apple calli and *Arabidopsis*

The full-length *MdABCG25* cDNA sequences were cloned from 'Royal Gala' apple tissue-cultured seedlings into the pRI-101-GFP plant expression plasmid downstream of the cauliflower mosaic virus (CaMV) 35S promoter using homologous recombination method. The primers are shown in Supplemental Table S1. *MdABCG25* overexpressed and RNAi vectors were transformed into Agrobacterium tumefaciens LBA4404 and GV3101. Transgenic *Arabidopsis* with *MdABCG25* ectopically expressed and transgenic apple calli were obtained by agrobacterium-mediated method[11].

RNA extraction and real-time quantitative RT-qPCR analysis

The total RNA of plant materials (including tissues of 'Royal Gala' apple trees, tissue-cultured apple seedlings, apple calli, and leaves of *Arabidopsis*) were extracted using the OminiPlant RNA Kit (Dnase I, ComWin Biotech Co., Ltd., Beijing, China) under RNase-free conditions. The cDNA as the template of RT-qPCR was obtained using the MonScript™ RTIII All-in-One Mix with dsDNase (Monad Biotech Co., Ltd., Wuhan, China). *18s* rRNA and *AtACTIN* rRNA were used as internal reference genes of apple and *Arabidopsis*, respectively. The RT-qPCR was performed by UltraSYBR Mixture (Low ROX) (ComWin Biotech Co., Ltd., Beijing, China) and $2^{-\Delta\Delta C_T}$ calculation method. Quantitative correlation primers are shown in Supplemental Table S1.

Toluidine blue (TB) staining, water loss assays, and chlorophyll leaching assays

All experiment were performed with the five-week-old *Arabidopsis*. The inflorescences, stems and rosette leaves of *Arabidopsis* were stained in the 0.05% TB staining solution for 10 h at room temperature. Rinse all samples with deionized water at least three times[12].

The rosette leaves of *Arabidopsis* were cut and weighed every 30 min until 150 min, and then the water loss rate was calculated.

The rosette leaves of *Arabidopsis* were weighed and placed into 50 mL tubes containing 40 mL 80% ethanol solution at 25 °C in the dark. One mL was taken from the sample tubes at 10, 30, 60, 120, and 180 min for spectrophotometer measurement[13].

The absorbance of each sample was measured at 649 nm and 665 nm respectively, and the formula is as follows:

Chlorophyll concentration in the extracting solution (C) = $6.63A_{665} + 18.08A_{649}$

Chlorophyll content (mg·g^{-1} FW) = (C * V)/FW

Extraction of cuticular waxes and component analysis by gas chromatography–mass spectrometry (GC-MS)

The stems and rosette leaves of *Arabidopsis* at five weeks of age with cauline leaves and siliques removed were cut off and weighed. Then their areas were measured, and their cuticular waxes were extracted with chloroform.

Each sample was replicated three times. The stems and rosette leaves were immersed in 20 mL chloroform for 30 s and repeated three times until all the wax was dissolved[14–16].

N, O-bis (trimethylsilyl) trifluoroacetamide (BSTFA, Sigma) was added and the derivatization reaction was carried out at 70 °C for 60 min with oscillation. Then BSTFA was dried by N_2. The sample was redissolved in chloroform and N-tetracosane (C24 alkane) was added as internal standard for gas chromatography-mass spectrometry (Shimadzu, Japan) analysis[17].

Scanning electron microscopy (SEM)

The five-week-old *Arabidopsis* rosette leaves and stems were rapidly frozen with liquid nitrogen and freeze-dried in vacuum for 24 h (FDU-1110, TOKYO RIKAKIKAI CO LTD, Japan, 50/60 Hz, 1.7kVA). Subsequently, they were fixed to metal plates and sprayed with gold following the procedure described in Qi et al[18]. The epidermal wax crystals were observed using a scanning electron microscope (SEM, JSM-6610LV, JEOL, Tokyo, Japan) at 5 kV.

Physiological measurements of apple calli and *Arabidopsis* under PEG 6000, NaCl and ABA treatments

'Orin' apple calli were treated with 5% PEG 6000, 150 mmol·L^{-1} NaCl or 50 μmol·L^{-1} ABA for 20 d. Fresh weights, malondialdehyde (MDA) contents and relative conductivity were measured[19].

Arabidopsis seeds, including ecotype Columbia (Col-0) and *MdABCG25* ectopic expression transgenic lines, were sterilized with 75% ethanol and 15% NaClO and germinated on 1/2 MS medium after 2-d vernalization at 4 °C.

After 4 d, the seedings were transferred to 1/2 MS, 1/2 MS with 5% PEG 6000, 1/2 MS with 30 μmol·L^{-1} ABA or 1/2 MS with 150 mmol·L^{-1} NaCl. The root length and fresh weight of the seedlings were measured using ImageJ-win64 software and one in 10,000 electronic balance after 2 weeks.

After 7 d, the seedlings were grown in pots containing 80% medium vermiculite and 20% substrate of 7 cm × 7 cm × 9 cm. All pots were watered with the same amount to ensure the accuracy of the experiments. Seedlings were grown under normal moist environment for 15 d. Then, they were treated with drought for 20 d or 150 mmol·L^{-1} NaCl for 15 d, respectively. After 20 d, the group treated with drought stress was resumed watering for 2 d. Chlorophyll content, MDA content, H_2O_2 content and O_2^- content were measured according to the method of An et al[20].

Protein network relationship predictions of the AtABCG25 protein and MdABCG25 protein

The main interaction networks of the AtABCG25 and MdABCG25 protein were predicted using the online STRING database (http://string-db.org).

Data presentation and statistical analysis

Each result was based on three parallel experiments with at least three technical replicates to ensure the accuracy of the results. Error bars show the standard deviation (SD) of three

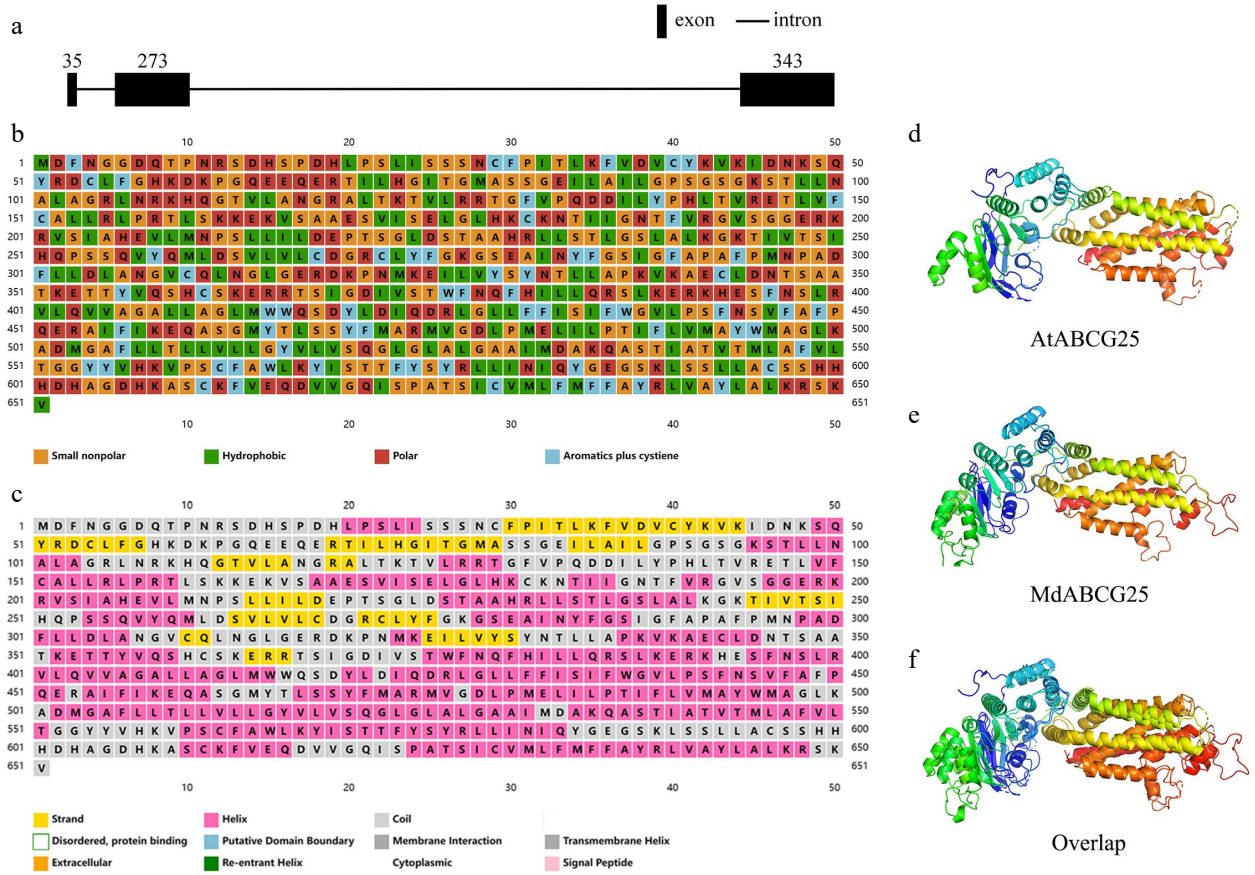

Fig. 1 Basic bioinformatic information about *AtABCG25* and *MdABCG25* sequence. (a) Genomic structure of *MdABCG25* sequence. The black rectangles denote exons, and the black lines denote introns. (b) Properties of each amino acid of MdABCG25 protein; orange for small nonpolar, green for hydrophobic, red for polar, and blue for aromatics plus cystiene. (c) Predicted secondary structures of MdABCG25 protein, each represented by a different color; yellow for strands, pink for helices, and gray for coils. The predicted tertiary structure of (d) AtABCG25 protein, (e) MdABCG25 protein, and their (f) overlaps.

replicates. All data were analyzed by IBM SPSS Statistics 20 software and compared using the single factor Duncan method. Treatment means with different lowercase letters are significantly different at $p < 0.05$.

Results

Bioinformatics analysis of the *MdABCG25* gene in apple

The apple *MdABCG25* (Md05G1042200) gene was identified in the apple genome by blasting the *Arabidopsis ABCG25* (AT1G71960) gene against the NCBI database. The full-length cDNA of *MdABCG25* was 1,956 bp in length, encoding 651 amino acids and containing three exons and two introns (Fig. 1a). Figure 1b showed the properties of each amino acid of MdABCG25 protein. *MdABCG25* gene was mapped to the 5th chromosome. Its predicted molecular weight is 71.78 kDa, and its predicted isoelectric point (pI) was 8.93. A maximum hydropathicity value of 3.233 and a minimum value of −3.100 were calculated by ProtScale, and the general average of hydropathicity of the protein was 0.135 (Supplemental Fig. S1a). The instability index was calculated at 36.45, which classified the protein as stable. Its aliphatic index was 99.62. MdABCG25

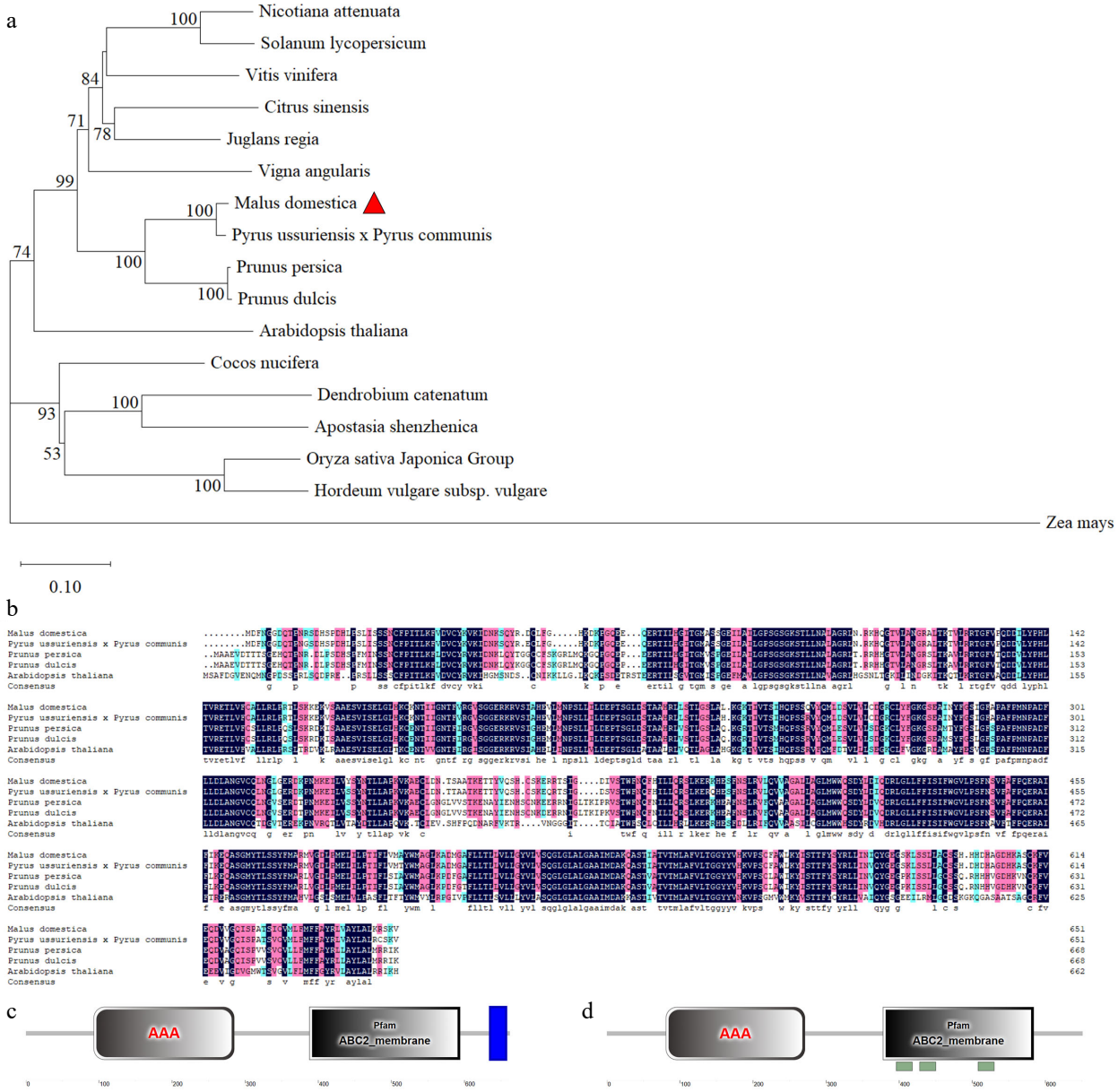

Fig. 2 Phylogenetic analysis, multiple sequence alignment and conserved motif analysis of ABCG25 proteins. (a) Phylogenetic tree assembled from ABCG25 proteins of 17 different species: *Nicotiana attenuate, Solanum lycopersicum, Vitis vinifera, Citrus sinensis, Juglans regia, Vigna angularis, Malus domestica, Pyrus ussuriensis* × *Pyrus communis, Prunus persica, Prunus dulcis, Arabidopsis thaliana, Cocos nucifera, Dendrobium catenatum, Apostasia shenzhenica, Oryza sativa Japonica Group, Hordeum vulgare subsp. Vulgare, Zea mays*. (b) Multiple sequence alignment of ABCG25 protein from different species: *Malus domestica*, *Pyrus* × *bretschneideri*, *Prunus persica*, *Prunus dulcis*, *Arabidopsis thaliana*. The conserved structural domains analysis of (c) AtABCG25 protein and (d) MdABCG25 protein sequences. The gray rectangles represent AAA domain. The blue rectangles represent transmembrane domain (TMD).

protein consisted of 44.85% alpha helices, 35.79% random coils, 14.59% extended strands and 4.76% beta turns (Fig. 1c, Supplemental Fig. S2). Based on the folding of the secondary structure, the tertiary structure of the AtABCG15 (Fig. 1d) and MdABCG25 protein (Fig. 1e) was predicted. There are six transmembrane domains, but no signal peptides were found (Supplemental Fig. S1b & c). The phosphorylation sites were predicted as follows: 41 serines, 19 threonines and six tyrosines (Supplemental Fig. S1d).

Phylogenetic analysis and conserved domain analysis of ABCG25 proteins from different species

To determine the phylogenetic relationship between MdABCG25 protein and ABCG25 in other species, we obtained 17 ABCG25 protein sequences, and constructed a phylogenetic tree by MEGA_64 software in order to compare these 17 protein sequences (Fig. 2a). The MdABCG25 protein (*Malus* × *domestica*) exhibited the closest evolutionary relationship with *Pyrus ussuriensis* × *Pyrus communis*, *Prunus persica*, and *Prunus dulcis*. The multiple sequence alignment showed that the homology of MdABCG25 to *Pyrus ussuriensis* × *Pyrus communis*, *Prunus persica*, and *Prunus dulcis* was 94.78%, 80.60%, and 80.15%, respectively (Fig. 2b). In addition, ZmABCG25 proteins (*Zea mays*) was most distant from MdABCG25.

The structural domains of AtABCG25 and MdABCG25 protein sequences were analyzed using the SMART website. They both contain a conserved AAA domain and an ABC2_membrane domain in a similar location (Fig. 2c & d). Furthermore, AtABCG25 has one more transmembrane domain (TMD) than MdABCG25, suggesting that they are ABCG half-sized transporters. The tertiary structures of AtABCG25 and MdABCG25 were predicted by the Phyre website. According to their tertiary structure merging results, the two structures strongly overlap (Fig. 1f). These results all showed that they may have similar functions.

Expression profiles in different apple tissues and promoter *cis*-acting element analysis of *MdABCG25*

In previous studies, many genes related to cuticular wax were highly expressed in apple pericarp[11,13,16,19,21,22]. To examine tissue-specific expression of *MdABCG25*, its transcript levels were analyzed in apple root, leaf, flower, fruit, and pericarp using a quantitative RT-PCR assay. The findings showed that *MdABCG25* was expressed at different levels in all measured tissues. As shown in Fig. 3a, *MdABCG25* showed the highest expression in apple pericarp and lower expression in leaves and flowers, suggesting a potential specific function in apple fruit development.

Most ABCG transporters play an important role in response to various abiotic stresses[23–26]. To predict the putative functions of the *MdABCG25* genes in response to abiotic stresses, its 2,000 bp upstream of the transcription start site was analyzed. Potential *cis*-acting elements in *MdABCG25* promoter were determined by the PlantCARE website (Table 1). The promoter region of the *MdABCG25* gene contained various stress responsive elements, such as the drought inducibility element (MBS), the low-temperature response element (LTR), and the ABA response element (ABRE). The promoter sequence also contained multiple plant hormone response elements, such as the gibberellin-responsive element (P-box), the MeJA response element (CGTCA-motif), and the auxin-responsive element (TGA-element). These plant hormones are all related to the stress response of plants. Besides, an ACE, a light-responsive element, that can play a crucial part in plant growth and development was found in its promoter region.

Responses to the ABA, PEG 6000, and NaCl treatments of the *MdABCG25*

To confirm whether *MdABCG25* gene responds to abiotic stresses in apple, *MdABCG25* transcription levels were measured in the tissue-cultured 'Royal Gala' apple seedlings under

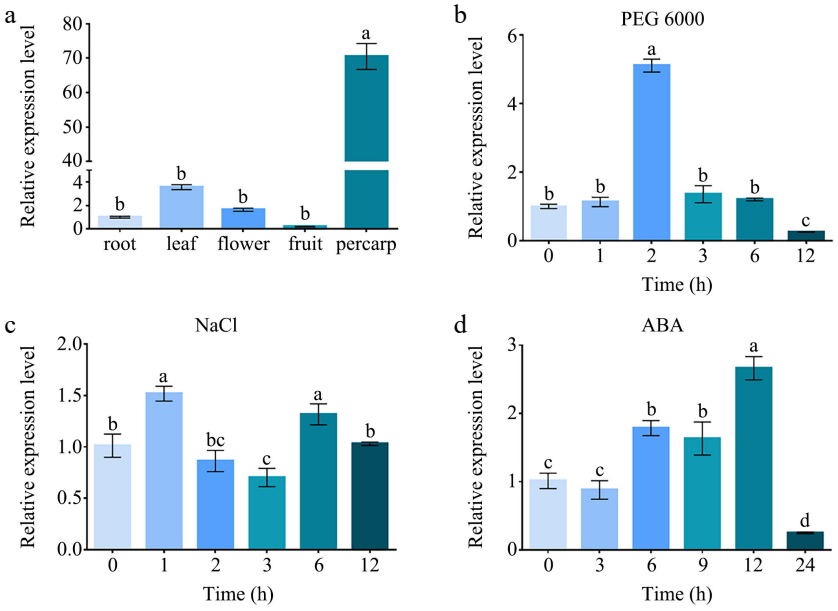

Fig. 3 The relative expression analysis of MdABCG25. (a) The relative expression levels of *MdABCG25* in apple root, leaf, flower, fruit, pericarp measured by RT-qPCR. The relative expression levels of *MdABCG25* under different stress treatments: (b) 10% PEG 6000, (c) 100 mmol·L^{-1} NaCl, and (d) 100 μmol·L^{-1} ABA measured by RT-qPCR. Data are mean ± SD of three independent replicates. Different lowercase letters indicate a significant difference at $p < 0.05$.

PEG 6000, NaCl or ABA treatments using RT-qPCR (Fig. 3b & d). We found that the expression of *MdABCG25* gene showed an increase-decrease trend under three abiotic stress conditions. The relative *MdABCG25* expression levels were up-regulated dramatically at 2 h and then decreased in response to the PEG 6000 treatment. The expression of *MdABCG25* fluctuated, and peaked at 1 h and 6 h in response to the NaCl treatment. The *MdABCG25* expression rose initially, peaked at 12 h, and then declined in response to the ABA treatment. These results suggested that *MdABCG25* may be involved in responding to various abiotic stresses.

Moreover, we obtained *MdABCG25* overexpressed (*MdABCG25*-OE), and suppressed (*MdABCG25*-RNAi) apple calli. The relative expression levels of *MdABCG25* in transgenic apple calli were measured using RT-qPCR (Fig. 4b). The 15-day-old apple calli were subcultured on MS medium, 5% PEG 6000, 150 mM NaCl or 50 μM ABA treatments (Fig. 4a). The results showed there were no significant differences in fresh weight among *MdABCG25*-OE line, *MdABCG25*-RNAi line and WT apple calli on MS medium (Fig. 4c). However, the fresh weight of the *MdABCG25*-OE line significantly increased compared to that of the WT apple calli, whereas the fresh weight of the

Table 1. *MdABCG25* promoter *cis*-acting element analysis.

Cis-element name	Sequence	Function	Start site (bp)	Termination site (bp)
P-box	CCTTTTG	Gibberellin-responsive element	271	277
MBS	CAACTG	MYB binding site involved in drought-inducibility	531	536
CGTCA-motif	CGTCA	*cis*-acting regulatory element involved in the MeJA-responsiveness	723	727
LTR	CCGAAA	*cis*-acting element involved in low-temperature responsiveness	1,122	1,127
TGA-element	AACGAC	Auxin-responsive element	1,324	1,329
ACE	CTAACGTATT	*cis*-acting element involved in light responsiveness	1,458	1,467
ABRE	ACGTG	*cis*-acting element involved in the abscisic acid responsiveness	1,856	1,860

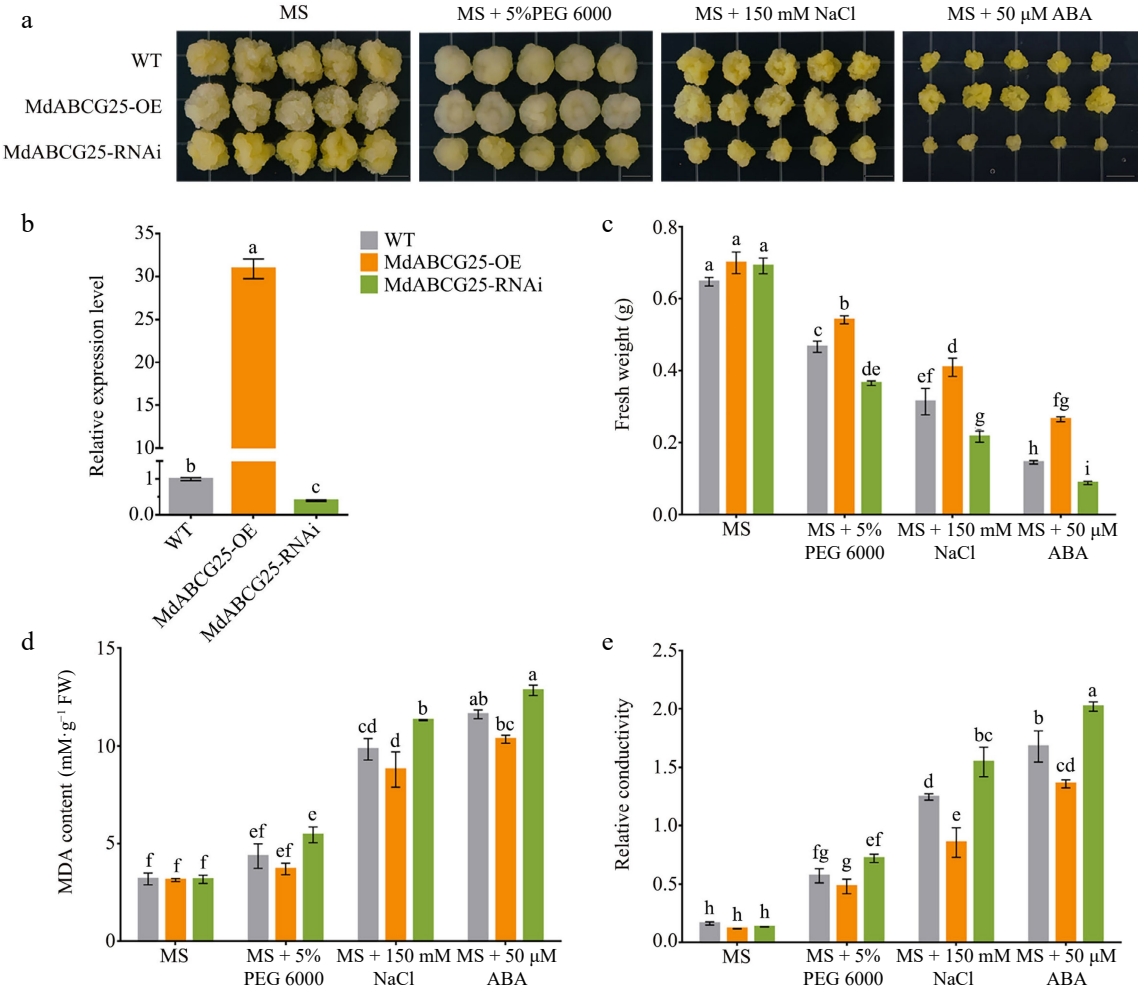

Fig. 4 Phenotypes of *MdABCG25* transgenic apple calli under different abiotic stress conditions. (a) Phenotypes of *MdABCG25* transgenic lines and wild-type (WT) apple calli treated with MS medium, MS + 5% PEG 6000, MS + 150 mmol·L^{-1} NaCl and MS + 50 μmol·L^{-1} ABA. (b) Relative expression levels of *MdABCG25* in wild-type (WT) apple calli and *MdABCG25* transgenic lines measured by RT-qPCR. (c) Fresh weight, (d) MDA content and (e) relative conductivity of *MdABCG25* transgenic lines and WT apple calli after treatments. FW = fresh weight. Data are mean ± SD of three independent replicates. Different lowercase letters indicate a significant difference at $p < 0.05$.

MdABCG25-RNAi line significantly decreased compared to that of WT under PEG 6000, NaCl and ABA treatment. MDA content and relative conductivity showed opposite changes, indicating that the damage of apple calli under abiotic stresses was reduced with the increase of *MdABCG25* expression level (Fig. 4d & e). These results suggest that *MdABCG25* plays a vital role in the response to abiotic stresses in apple. In addition, overexpression of *MdABCG25* decreased the sensitivity of apple calli to ABA.

MdABCG25 reduced epidermal permeability in *Arabidopsis*

To investigate the function of *MdABCG25* in plants, we obtained three *MdABCG25* transgenic *Arabidopsis* (*MdABCG25*-OE-1, *MdABCG25*-OE-2, *MdABCG25*-OE-3), and measured *MdABCG25* transcription levels using RT-qPCR (Fig. 5b). To explore whether epidermal permeability was altered in *MdABCG25* transgenic *Arabidopsis*, the inflorescences, stems, and leaves of *MdABCG25* transgenic lines and Col-0 was stained with TB (Fig. 5a). The results of TB staining showed that inflorescence, stems and leaves of Col-0 were more easily stained than those of *MdABCG25* transgenic *Arabidopsis*. The epidermal permeability of *MdABCG25* transgenic lines was lower than that of Col-0. Moreover, it was found that the rosette leaves of *MdABCG25* transgenic lines had lower water loss rates and chlorophyll extractions compared with Col-0 through water loss and chlorophyll extraction experiment (Fig. 5c & d). In conclusion, we hypothesized that *MdABCG25* may reduce plant epidermal permeability by promoting wax transport, suggesting a potential impact on plant drought resistance.

MdABCG25 promoted cuticular wax accumulation

To study the function of *MdABCG25* in wax transport, we tested the expression of wax-related genes in *MdABCG25* transgenic *Arabidopsis* and Col-0. Some genes were up-regulated in transgenic *Arabidopsis* compared with Col-0, including *AtCER1*, *AtACBP1*, *AtECH* and *AtKCS1* (Supplemental Fig. S3). Furthermore, the content and composition of cuticular wax in the *Arabidopsis* stems were determined (Fig. 6). There were significant differences in total wax load between *MdABCG25* transgenic *Arabidopsis* and Col-0, both on leaves and stems (Fig. 6a & b). In addition, the wax components in stems were analyzed by gas chromatography-mass spectrometry (GC-MS). The cuticular wax composition of *MdABCG25* transgenic *Arabidopsis* was significantly different from that of Col-0, and the contents of alkanes, alcohols, aldehydes and ketones were significantly increased (Fig. 6c–h). Among alkanes, *MdABCG25* transgenic *Arabidopsis* has more C29 alkane and C31 alkane (Fig. 6f). The contents of C30 aldehyde, C26 and C28 alcohols were much higher in *MdABCG25* transgenic lines than in Col-0 (Fig. 6e & h). However, the levels of fatty acids decreased in *MdABCG25* transgenic *Arabidopsis*, such as palmitic acid and stearic acid (Fig. 6g).

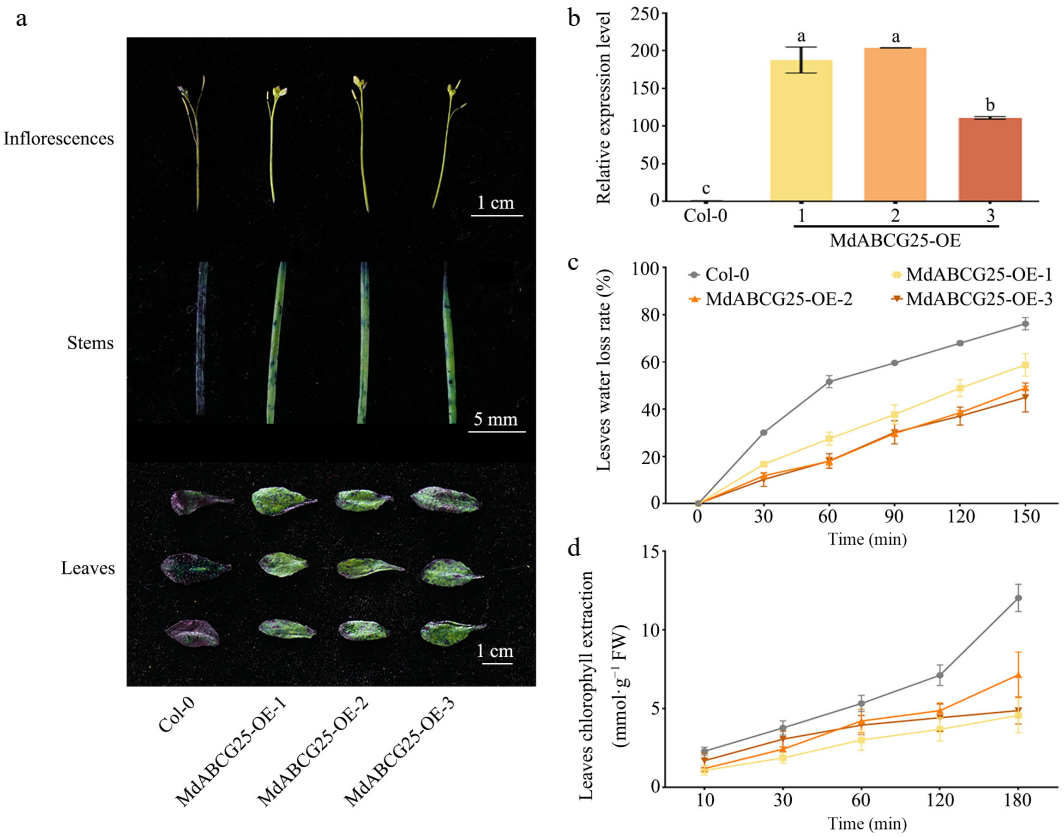

Fig. 5 *MdABCG25* can reduce the epidermis permeability of *Arabidopsis*. (a) TB staining of inflorescences, stems and leaves of the *MdABCG25* transgenic lines and Col-0. Scale bars correspond to 1 cm, 5 mm and 1 cm, respectively. (b) Expression levels of *MdABCG25* in three *MdABCG25* transgenic *Arabidopsis* and Col-0 using RT-qPCR analysis. (c) Water loss rate of rosette leaves of the *MdABCG25* transgenic lines and Col-0. (d) Chlorophyll extraction of rosette leaves of the *MdABCG25* transgenic lines and Col-0. Data are mean ± SD of three independent replicates. Different lowercase letters indicate a significant difference at $p < 0.05$.

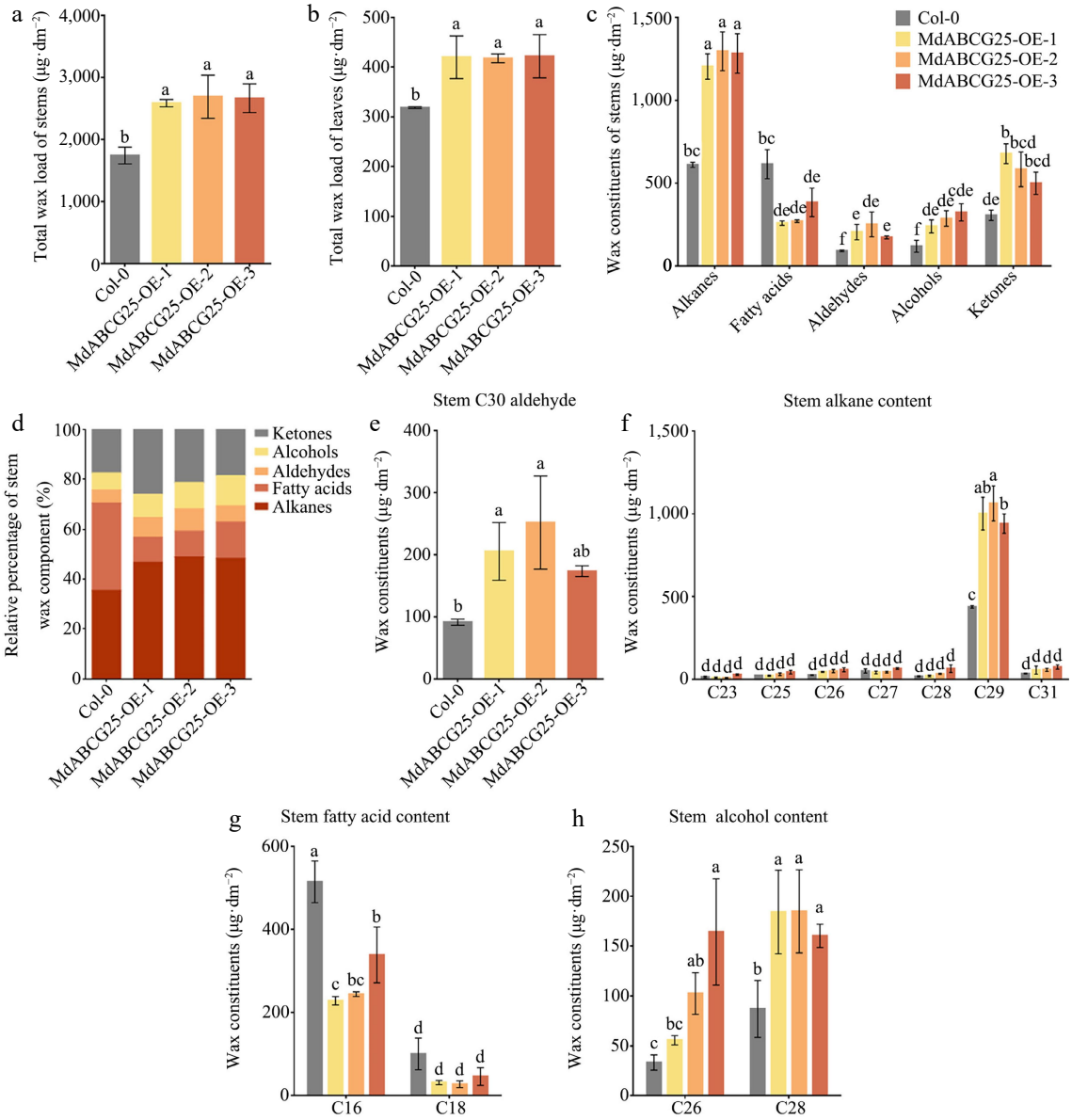

Fig. 6 The effect of *MdABCG25* on cuticular wax content and composition. Total wax load of (a) stems and (b) leaves of the *MdABCG25* transgenic *Arabidopsis* and Col-0. (c) Wax composition of stems of the *MdABCG25* transgenic *Arabidopsis* and Col-0 analyzed by GC-MS. (d) Relative percentage of stems wax component. Stem wax constituents of (e) aldehydes, (f) alkanes, (g) fatty acids and (h) alcohols in *MdABCG25* transgenic *Arabidopsis* and Col-0 analyzed by GC-MS. The compounds were tentatively identified by GC-MS solution software. Data are mean ± SD of three independent replicates. Different lowercase letters indicate a significant difference at $p < 0.05$.

In addition, we observed the epidermis ultrastructure of the *MdABCG25* transgenic and Col-0 *Arabidopsis* stems and leaves using SEM (Fig. 7). The wax crystals and wax plates of *MdABCG25* transgenic *Arabidopsis* epidermis were significantly larger and more than those of Col-0, especially the long strip wax crystals increased observably (Fig. 7a & b). These results indicated that the expression of *MdABCG25* affected the chemical composition and ultrastructure of plants cuticular wax.

MdABCG25 increased *Arabidopsis* resistance to abiotic stress

To investigate whether the increase of epidermal wax load caused by *MdABCG25* can enhance the resistance plant to abiotic stresses, Col-0 and *MdABCG25* transgenic *Arabidopsis* seeding were transferred to 1/2 MS medium containing 30μmol·L^{-1} ABA, 5% PEG 6000, or 150 mmol·L^{-1} NaCl (Fig. 8a). Under normal conditions, the root length of *MdABCG25* transgenic lines was slightly larger than Col-0, but there was no significant difference in fresh weight (Fig. 8b). Under the PEG 6000 or NaCl treatment, *MdABCG25* transgenic lines showed obviously longer primary roots and greater fresh weight than Col-0 (Fig. 8b & c). Under the ABA treatment, the *MdABCG25* transgenic lines showed only a slight increase in root length and fresh weight. In addition, the *MdABCG25* transgenic lines showed longer and more lateral roots than Col-0 *Arabidopsis* under PEG 6000 and NaCl treatments (Fig. 8a). These results suggest that ectopic expression of *MdABCG25* not only enhances the resistance of *Arabidopsis* to abiotic stresses but decreases plant sensitivity to ABA.

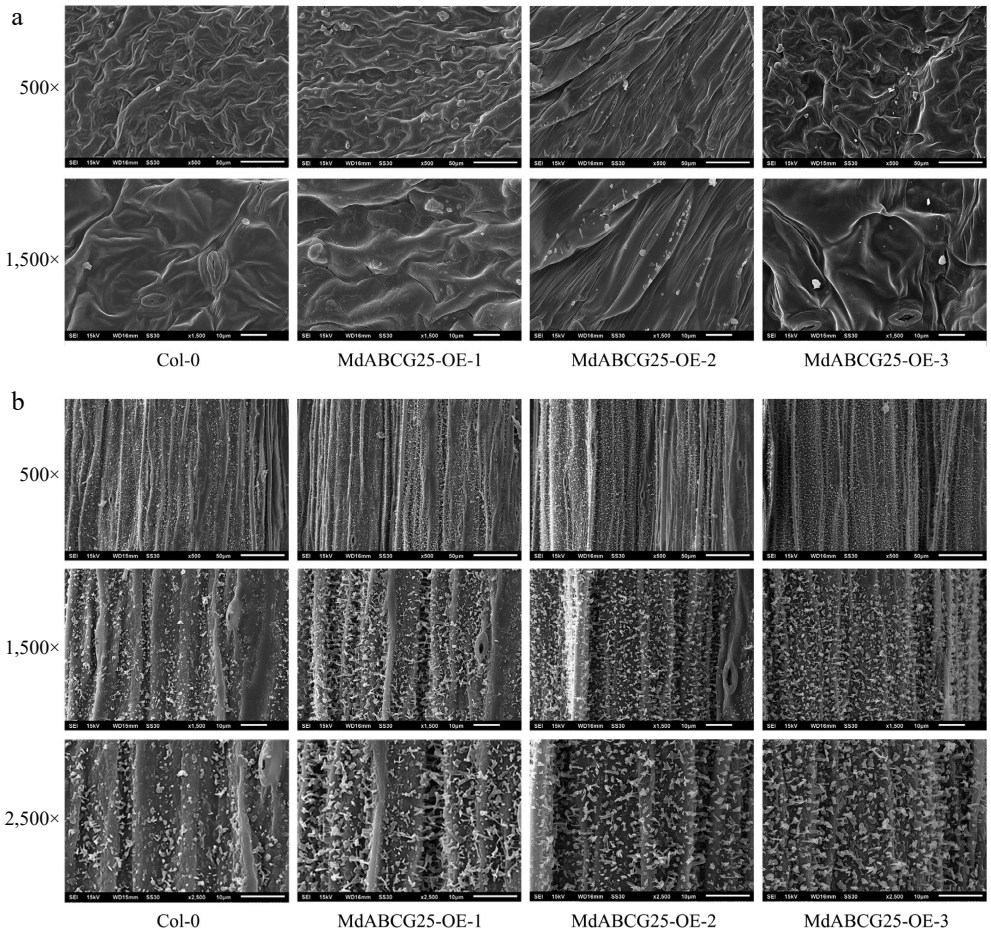

Fig. 7 Cuticle wax crystal morphology of *MdABCG25* transgenic and Col-0 *Arabidopsis* observed by SEM. The epidermal ultrastructure of *MdABCG25* transgenic and Col-0 *Arabidopsis* rosette (a) leaves and (b) stems. Wax crystals were monitored at 500×, 1,500× and 2,500× magnification, and scale bars correspond to 50 μm, 10 μm and 10 μm, respectively.

To further verify the resistance of *MdABCG25* transgenic to drought and salt stress at seedling stage, the healthy 3-week-old *MdABCG25* transgenic and Col-0 *Arabidopsis* seedlings were treated by drought for 20 d or 150 mmol·L^{-1} NaCl for 15 d, respectively (Fig. 9a & f). After 20 d, the drought stress treatment group was resumed watering for 2 d. Under the drought or NaCl treatment, the growth of both transgenic lines and Col-0 was inhibited, but the degree of growth inhibition of transgenic lines was significantly lower than that of Col-0. The *MdABCG25* transgenic seedings were more robust than Col-0, with significantly fewer dry rosette leaves. The chlorophyll content of *MdABCG25* transgenic lines was higher than that of Col-0 *Arabidopsis* (Fig. 9b & g). Moreover, *MdABCG25* transgenic seedings showed lower MDA, H_2O_2 and O_2^- contents than Col-0 under both drought and NaCl treatments (Fig. 9c–e & h–j).

Protein interaction network predictions for the AtABCG25 protein and MdABCG25 protein

In order to further identify the regulating pathway of *MdABCG25* in cuticular wax transport and alleviating abiotic stresses, we predicted the protein interaction network of AtABCG25 and MdABCG25 proteins (Fig. 10). MdABCG25 was predicted to interact with ethylene related proteins, such as ETR1b, ERS, ERS2, and ETR1, indicating that MdABCG25 may be involved in regulating fruit ripening and plant aging. XP_008389536.1, XP_008389530.1, and XP_008339944.1, which were NRT1/ PTR family 4.6-like proteins, were predicted to interact with MdABCG25 (Fig. 10b). In the network of AtABCG25 protein, ABCD1 is related to transport of lipids and fatty acid. F12K2.4 affects the cell wall structure. ETR1 and ERS1 are related to ethylene. NCED3 and ABA4 are related to abscisic acid. NRT1.1 is related to N absorption and transport. These interactions provide useful resources for further study of function of MdABCG25.

Discussion

The cuticular wax on the surface of apples not only protects the fruit by enhancing tolerance to biotic and abiotic stresses[16,27], but also improves surface gloss and storage capacity after harvest[28]. At present, the biosynthesis mechanism of the cuticular wax components is gradually being understood[29]. However, the mechanism by which the cuticular wax components are exported from epidermal cells and assembled into complex, three-dimensional, hydrophobic plant surface structures is still unclear. In this work, we cloned and characterized the full-length *MdABCG25*, encoding a half-sized ABCG subfamily transporter, and studied its properties, aiming to reveal its function in the cuticular wax transport and the adaptation to extreme environments in apple.

In epidermal cells, wax components must be transported from the biosynthesis site of the endoplasmic reticulum to the

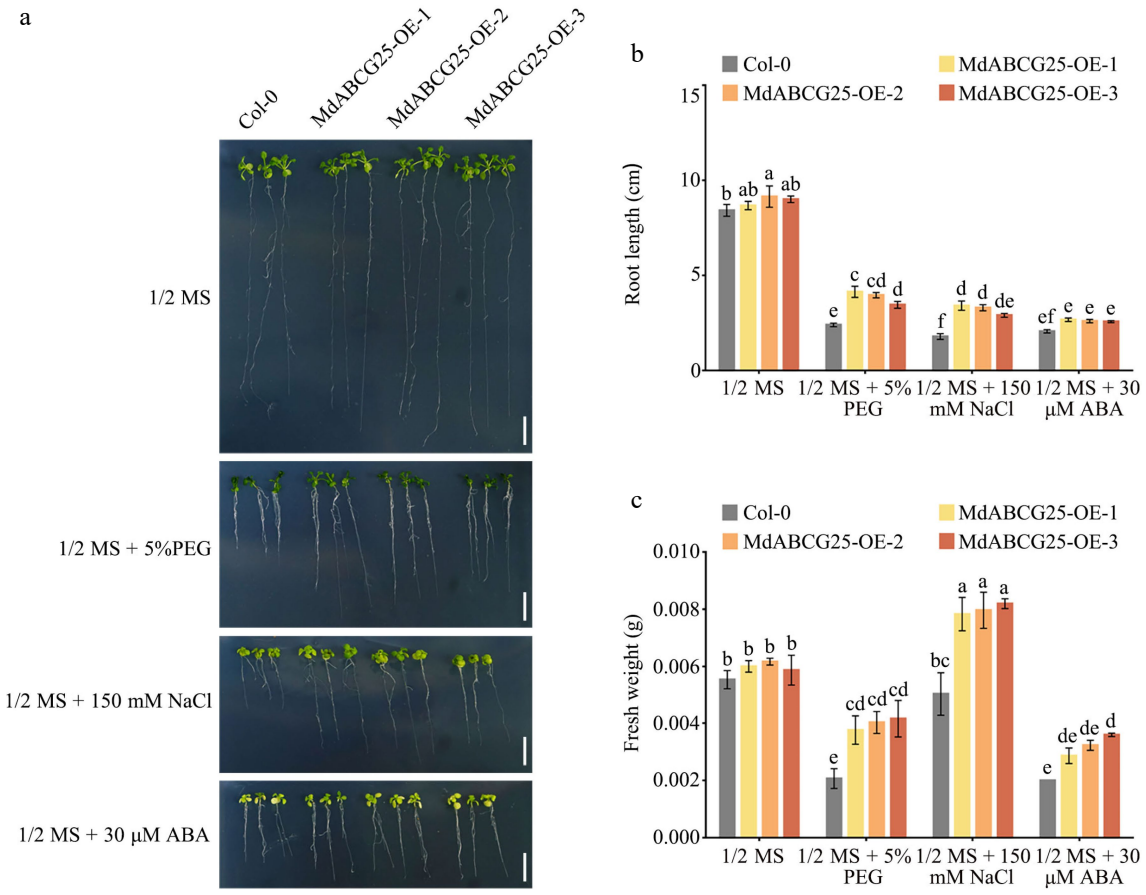

Fig. 8 Phenotypes of *MdABCG25* transgenic and Col-0 *Arabidopsis* seedings under different abiotic stress conditions. (a) Phenotypes of *MdABCG25* transgenic and Col-0 *Arabidopsis* seedings treated with 1/2 MS medium, 1/2 MS + 5% PEG 6000, 1/2 MS + 150 mmol·L^{-1} NaCl and 1/2 MS + 30 μmol·L^{-1} ABA. Bar = 1 cm. (b) Root length and (c) fresh weight of *MdABCG25* transgenic and Col-0 *Arabidopsis*. FW = fresh weight. Data are mean ± SD of three independent replicates. Different lowercase letters indicate a significant difference at $p < 0.05$.

plasma membrane (PM), through PM, and finally through the cell wall to the stratum corneum. The transport of wax components from the ER to PM can be accomplished through three possible pathways: direct transport at the physical contact sites between the ER and the PM[30], transport *via* cytoplasmic carrier proteins[31], and vesicle transport[31,32]. After transporting the wax components to the PM, they must pass through the lipid bilayer to enter the apoplast. Studies have found that the ABCG transporter protein was involved in this process. The ABCG subfamily is divided into half-sized transporters (WBC) and full-sized transporters (PDR)[33]. WBC must form dimers to exert transport activity[33,34]. AtABCG11 half-sized transporters can form dimers to transport different wax precursors or cutin precursors with itself, AtABCG12, AtABCG5, AtABCG9, or AtABCG14, respectively[34–37]. *MdABCG25* showed the highest expression in apple pericarp, suggesting that *MdABCG25* may be involved in transport of cuticular wax in apple. Therefore, we suspect that *MdABCG25*, as a half-sized ABCG transporters, may combine with itself or other half-sized ABCG transporters to form homodimers or heterodimers to export different substrates.

Previous studies have shown that overexpression of *TsABCG11* increases cuticular wax accumulation and abiotic stress resistance in *Arabidopsis*[38]. The promoter region of the *MdABCG25* gene contained various stress responsive elements, further suggesting that *MdABCG25* may also be involved in the plant stress response. The GC-MS analysis of wax showed heterologous expression of *MdABCG25* in *Arabidopsis* can promote cuticular wax transport to resist drought and salt stress. Meanwhile, *MdABCG25* transgenic *Arabidopsis* seedlings also showed stronger resistance to drought and salt stress in the tissue-cultured environment, even if only a small amount of cuticular wax was accumulated, suggesting that *MdABCG25* can enhance plant resistance by up-regulating the expression of resistance genes in addition to increasing wax accumulation.

The results of this study indicate that overexpression of *MdABCG25* not only improves drought resistance through stomatal-independent pathway, but also through stomatal-dependent pathway. However, these results contradict that *MdABCG25* is insensitive to ABA shown by Figs 4 & 8. The plant hormone ABA, as an endogenous messenger in plants responding to biotic and abiotic stresses, plays an important role in the regulation of water loss[39]. Drought leads to a strong increase in plant ABA levels, inducing stomatal closure of protective cells and accompanied by major changes in gene expression in order to resist drought stress[40]. Similarly, some wax-related genes, *MdKCS2* and *MdLACS2*, are insensitive to ABA and can enhance drought resistance[21,22]. It is speculated that wax-related genes may also participate in improving drought resistance through an ABA-independent pathway. Moreover, overexpression of *AtABCG25*, ABA exporter, resulted in plant insensitivity to ABA and increased drought resistance[24]. NCED3 and ABA4, being related to ABA, are predicted to interact with MdABCG25 (Fig. 10b). Therefore, *MdABCG25* may have the

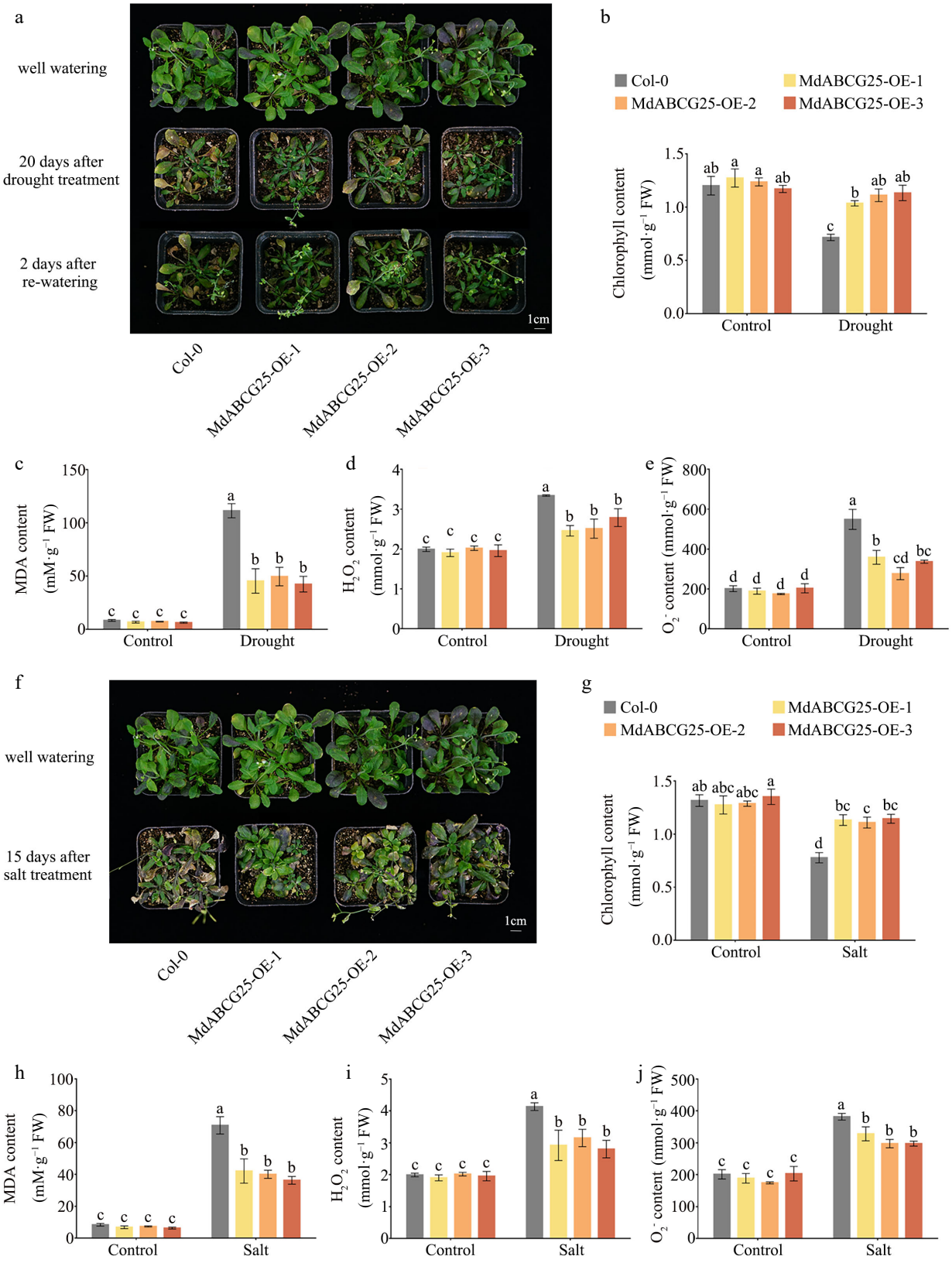

Fig. 9 *MdABCG25* can enhance tolerance to drought and salt in *Arabidopsis*. (a) Phenotypes of *MdABCG25* transgenic and Col-0 *Arabidopsis* in normal conditions or 20 d of drought treatment. Physiological indicators in *MdABCG25* transgenic and Col-0 *Arabidopsis* in normal conditions and drought treatment; (b) chlorophyll content, (c) MDA content, (d) O_2^- content, (e) H_2O_2 content. (f) Phenotypes of *MdABCG25* transgenic and Col-0 *Arabidopsis* in normal conditions or 15 d of 100 mmol·L^{-1} NaCl treatment. Physiological indicators in *MdABCG25* transgenic and Col-0 *Arabidopsis* in normal conditions and salt treatment; (g) chlorophyll content, (h) MDA content, (i) O_2^- content, (j) H_2O_2 content. Values are mean ± SD of at least three biological replicates. Different lowercase letters indicate a significant difference at $p < 0.05$.

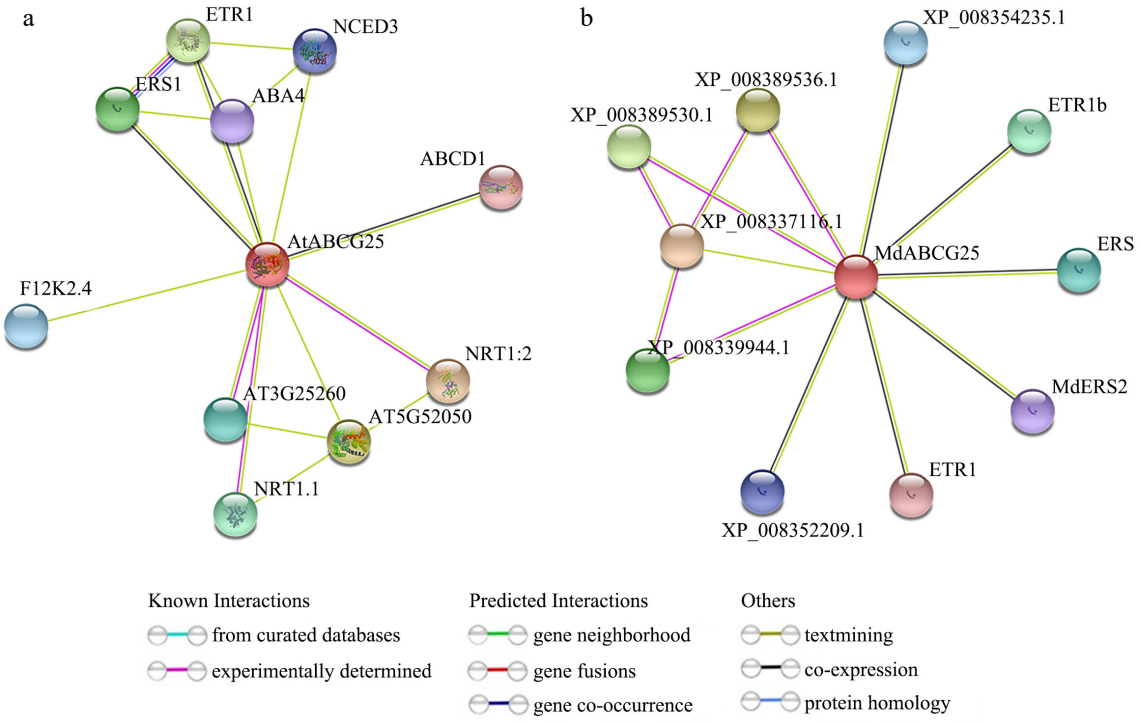

Fig. 10 Protein interaction networks for the AtABCG25 and MdABCG25 proteins. Predicted interaction networks for the (a) AtABCG25 and (b) MdABCG25 proteins generated using the online software STRING.

same function. These conjectures need to be confirmed in future studies.

Although ABCG transporters have been proved to be involved in extracellular accumulation of wax molecules, the detailed biochemical processes behind transport events have not been determined[41]. The characteristics and functions of ABCG transporters have mostly been reported based on molecular genetic methods, in which the transport mechanism is still unknown[42]. Moreover, heterodimerization of half-sized ABCG family members provides great potential to identify a plenty of substrates for transport, but this also affects the specificity of transport substrates.

In conclusion, the process of wax transport in plant epidermis is very complicated, and there are many genes involved in this process, so it is difficult to study the genes involved in wax transport in plant epidermis. In this paper, *MdABCG25* gene in apple was cloned and identified, and its characteristics were studied. *MdABCG25* gene promotes the accumulation of plant cuticular wax, reduces the permeability of plant epidermis, and improves the drought resistance and salt resistance of plants. It laid a foundation for elucidating the molecular mechanism of plant wax transport in apple, and provided candidate genes for improving abiotic stress tolerance and fruit quality of apple.

Author contributions

The authors confirm contribution to the paper as follows: Li YY, Han J, Lv YH designed the idea of the research; Zhou MM performed the experiments, collected data, analyzed and interpreted results, and prepared draft manuscript; Yu ZH, Gao HN, Li MR, Wu YT, Li HY, Wang T assisted in experiments. All authors reviewed the results and approved the final version of the manuscript.

Data availability

All data generated or analyzed during this study are included in this published article and its Supplemental information files.

Acknowledgments

This work was supported by the National Natural Science Foundation of China (32072539), Natural Science Foundation of Shandong Province (ZR2022JQ14 and ZR2022QC112) and Taishan Scholar Young Expert Program.

Conflict of interest

The authors declare that they have no conflict of interest.

Supplementary Information accompanies this paper at (https://www.maxapress.com/article/doi/10.48130/FruRes-2023-0043)

Dates

Received 14 September 2023; Accepted 17 November 2023; Published online 15 December 2023

References

1. Hansjakob A, Bischof S, Bringmann G, Riederer M, Hildebrandt U. 2010. Very-long-chain aldehydes promote *in vitro* prepenetration processes of *Blumeria graminis* in a dose- and chain length-dependent manner. *New Phytologist* 188:1039–54
2. Castillo L, Diaz M, González-Coloma A, González A, Alonso-Paz E, et al. 2010. *Clytostoma callistegioides* (Bignoniaceae) wax extract with activity on aphid settling. *Phytochemistry* 71:2052–57

3. Schreiber L. 2010. Transport barriers made of cutin, suberin and associated waxes. *Trends in Plant Science* 15:546–53
4. Buda GJ, Barnes WJ, Fich EA, Park S, Yeats TH, et al. 2013. An ATP binding cassette transporter is required for cuticular wax deposition and desiccation tolerance in the moss *Physcomitrella patens*. *The Plant Cell* 25:4000–13
5. Pighin JA, Zheng H, Balakshin LJ, Goodman IP, Western TL, et al. 2004. Plant cuticular lipid export requires an ABC transporter. *Science* 306:702–4
6. Panikashvili D, Shi JX, Schreiber L, Aharoni A. 2011. The Arabidopsis ABCG13 transporter is required for flower cuticle secretion and patterning of the petal epidermis. *New Phytologist* 190:113–24
7. Zhao G, Shi J, Liang W, Xue F, Luo Q, et al. 2015. Two ATP binding cassette G transporters, rice ATP binding cassette G26 and ATP binding cassette G15, collaboratively regulate rice male reproduction. *Plant Physiology* 169:2064–79
8. Bessire M, Borel S, Fabre G, Carraça L, Efremova N, et al. 2011. A member of the PLEIOTROPIC DRUG RESISTANCE family of ATP binding cassette transporters is required for the formation of a functional cuticle in *Arabidopsis*. *The Plant Cell* 23:1958–70
9. Yang Z, Zhang T, Lang T, Li G, Chen G, et al. 2013. Transcriptome comparative profiling of barley eibi1 mutant reveals pleiotropic effects of *HvABCG31* gene on cuticle biogenesis and stress responsive pathways. *International Journal of Molecular Sciences* 14:20478–91
10. Li L, Li D, Liu S, Ma X, Dietrich CR, et al. 2013. The maize *glossy13* gene, cloned via BSR-Seq and Seq-Walking encodes a putative ABC transporter required for the normal accumulation of epicuticular waxes. *PLoS ONE* 8:e82333
11. Zhang C, Wang Y, Hu X, Zhang Y, Wang G, et al. 2020. An apple AP2/EREBP-type transcription factor, *MdWRI4*, enhances plant resistance to abiotic stress by increasing cuticular wax load. *Environmental and Experimental Botany* 180:104206
12. de Campos Vidal B, Mello MLS. 2019. Toluidine blue staining for cell and tissue biology applications. *Acta Histochemica* 121:101–12
13. Zhang Y, Zhang C, Wang G, Wang Y, Qi C, et al. 2019. Apple AP2/EREBP transcription factor MdSHINE2 confers drought resistance by regulating wax biosynthesis. *Planta* 249:1627–43
14. Pham TCT, Angers P, Ratti C. 2018. Extraction of wax-like materials from cereals. *The Canadian Journal of Chemical Engineering* 96:2273–81
15. Ardenghi N, Mulch A, Pross J, Niedermeyer EM. 2017. Leaf wax *n*-alkane extraction: an optimised procedure. *Organic Geochemistry* 113:283–92
16. Li J, Zhang C, Zhang Y, Gao H, Wang H, et al. 2022. An apple long-chain acyl-CoA synthase, *MdLACS1*, enhances biotic and abiotic stress resistance in plants. *Plant Physiology and Biochemistry* 189:115–25
17. Lü S, Song T, Kosma DK, Parsons EP, Rowland O, et al. 2009. Arabidopsis *CER8* encodes LONG-CHAIN ACYL-COA SYNTHETASE 1 (LACS1) that has overlapping functions with LACS2 in plant wax and cutin synthesis. *The Plant Journal* 59:553–64
18. Qi C, Zhao X, Jiang H, Zheng P, Liu H, et al. 2019. Isolation and functional identification of an apple *MdCER1* gene. *Plant Cell, Tissue and Organ Culture (PCTOC)* 136:1–13
19. Zhang C, Mao K, Zhou L, Wang G, Zhang Y, et al. 2018. Genome-wide identification and characterization of apple long-chain Acyl-CoA synthetases and expression analysis under different stresses. *Plant Physiology and Biochemistry* 132:320–32
20. An J, Wang X, Yao J, Ren Y, You C, et al. 2017. Apple MdMYC2 reduces aluminum stress tolerance by directly regulating MdERF3 gene. *Plant and Soil* 418:255–66
21. Lian X, Gao H, Jiang H, Liu C, Li Y. 2021. MdKCS2 increased plant drought resistance by regulating wax biosynthesis. *Plant Cell Reports* 40:2357–68
22. Zhang C, Hu X, Zhang Y, Liu Y, Wang G, et al. 2020. An apple *long-chain acyl-CoA synthetase 2* gene enhances plant resistance to abiotic stress by regulating the accumulation of cuticular wax. *Tree Physiology* 40:1450–65
23. Kang J, Hwang JU, Lee M, Kim YY, Assmann SM, et al. 2010. PDR-type ABC transporter mediates cellular uptake of the phytohormone abscisic acid. *Proceedings of the National Academy of Sciences of the United States of America* 107:2355–60
24. Kuromori T, Miyaji T, Yabuuchi H, Shimizu H, Sugimoto E, et al. 2010. ABC transporter AtABCG25 is involved in abscisic acid transport and responses. *Proceedings of the National Academy of Sciences of the United States of America* 107:2361–66
25. Li H, Li C, Sun D, Yang Z. 2024. OsPDR20 is an ABCG metal transporter regulating cadmium accumulation in rice. *Journal of Environmental Sciences* 136:21–34
26. Zhang H, Jing W, Zheng J, Jin Y, Wu D, et al. 2020. The ATP-binding cassette transporter OsPDR1 regulates plant growth and pathogen resistance by affecting jasmonates biosynthesis in rice. *Plant Science* 298:110582
27. Yang X, Zhao H, Kosma DK, Tomasi P, Dyer JM, et al. 2017. The acyl desaturase CER17 is involved in producing wax unsaturated primary alcohols and cutin monomers. *Plant Physiology* 173:1109–24
28. Zhang Y, You C, Li Y, Hao Y. 2020. Advances in biosynthesis, regulation, and function of apple cuticular wax. *Frontiers in Plant Science* 11:1165
29. Gan L, Wang X, Cheng Z, Liu L, Wang J, et al. 2016. Wax *crystal-sparse leaf 3* encoding a beta-ketoacyl-CoA reductase is involved in cuticular wax biosynthesis in rice. *Plant Cell Reports* 35:1687–98
30. McFarlane HE, Lee EK, Van Bezouwen LS, Ross B, Rosado A, et al. 2017. Multiscale structural analysis of plant ER-PM contact sites. *Plant and Cell Physiology* 58:478–84
31. Xue Y, Xiao S, Kim J, Lung SC, Chen L, et al. 2014. *Arabidopsis* membrane-associated acyl-CoA-binding protein ACBP1 is involved in stem cuticle formation. *Journal of Experimental Botany* 65:5473–83
32. Kunst L, Samuels AL. 2003. Biosynthesis and secretion of plant cuticular wax. *Progress in Lipid Research* 42:51–80
33. Dhara A, Raichaudhuri A. 2021. ABCG transporter proteins with beneficial activity on plants. *Phytochemistry* 184:112663
34. McFarlane HE, Shin JJH, Bird DA, Samuels AL. 2010. *Arabidopsis* ABCG transporters, which are required for export of diverse cuticular lipids, dimerize in different combinations. *The Plant Cell* 22:3066–75
35. Le Hir R, Sorin C, Chakraborti D, Moritz T, Schaller H, et al. 2013. ABCG9, ABCG11 and ABCG14 ABC transporters are required for vascular development in Arabidopsis. *The Plant Journal* 76:811–24
36. Elejalde-Palmett C, Martinez San Segundo I, Garroum I, Charrier L, De Bellis D, et al. 2021. ABCG transporters export cutin precursors for the formation of the plant cuticle. *Current Biology* 31:2111–2123.E9
37. Lee EJ, Kim KY, Zhang J, Yamaoka Y, Gao P, et al. 2021. *Arabidopsis* seedling establishment under waterlogging requires ABCG5-mediated formation of a dense cuticle layer. *New Phytologist* 229:156–72
38. Chen N, Song B, Tang S, He J, Zhou Y, et al. 2018. Overexpression of the ABC transporter gene *TsABCG11* increases cuticle lipids and abiotic stress tolerance in *Arabidopsis*. *Plant Biotechnology Reports* 12:303–13
39. Raghavendra AS, Gonugunta VK, Christmann A, Grill E. 2010. ABA perception and signalling. *Trends in Plant Science* 15:395–401
40. Hetherington AM. 2001. Guard cell signaling. *Cell* 107:711–14
41. Do THT, Martinoia E, Lee Y, Hwang JU. 2021. 2021 update on ATP-binding cassette (ABC) transporters: how they meet the needs of plants. *Plant Physiology* 187:1876–92
42. Gräfe K, Schmitt L. 2021. The ABC transporter G subfamily in *Arabidopsis thaliana*. *Journal of Experimental Botany* 72:92–106